World Journal of Advanced Research and Reviews
eISSN: 2581-9615 CODEN (USA): WJARAI
Cross Ref DOI: 10.30574/wjarr
Journal homepage: https://wjarr.com/

(RESEARCH ARTICLE)

Check for updates

Comparative study of the adsorption properties of several micropollutants on natural phosphate from Tahoua/Niger and activated carbon based on *Hyphaene thebaica* shells

AMADOU KIARI Mahamane Nassirou [1,*], SANDA MAMANE Ousmaila [2], I. HIMA Halidou [1], ZANGUINA Adamou [1], MALAM ALMA Maman Mousbahou [1] and NATATOU Ibrahim [1]

[1] *Laboratory of Materials, Water and Environment, Science and Technology Faculty, Abdou Moumouni University, BP: 10662 Niamey, Niger.*
[2] *National School of Engineering and Energy Sciences, University of Agadez, B.P: 199 Agadez, Niger.*

World Journal of Advanced Research and Reviews, 2025, 27(02), 1972-1983

Publication history: Received on 28 May 2025; revised on 20 July 2025; accepted on 27 July 2025

Article DOI: https://doi.org/10.30574/wjarr.2025.27.2.3024

Abstract

This study compares the adsorption properties of dyes on natural phosphate from Tahoua and activated carbon. The phosphate used is natural phosphate powder from Tahoua calcined at 850°C for two hours to increase the orthophosphate (P_2O_5) content. The activated carbons used were obtained from the shell of the *Hyphaene thebaica* (HT) nut by chemical activation with orthophosphoric acid (H_3PO_4) at 10% and 40% at a pyrolysis temperature of 450°C with an isothermal plateau of 1 hour 30 minutes. The shell was first characterized. The moisture content obtained was 5.002 %, the ash content was 5.828 % and the volatile matter content (loss on ignition) was 98.9587 %. The activated carbons produced (ACEs) have mass yields of around 42.85 % and 47.05 % when impregnated at 10% and 40%, respectively. Next, tests were conducted to determine the adsorption capacities of diiodine (I_2), methylene blue (MB), and methyl orange (MO) on the activated carbons produced (ACPs) and on natural phosphate from Tahoua (NPT). The results obtained show that the adsorption equilibrium time for methyl orange is 40 minutes and around 25 minutes for the developed activated carbon (CAE) and Tahoua natural phosphate (PNT), respectively. Finally, the surface functions and pH at zero charge point were determined using the Boehm method and the first bisector method, respectively. The surface functions of CAEs are acidic in nature and the pH at zero charge point is below neutrality. For Tahoua natural phosphate (PNT), the pH at zero charge point is slightly above neutrality.

Keywords: Adsorption; Activated Carbon; Iodine Index; Methylene Blue Index; Methyl Orange; Natural Phosphate from Tahoua

1. Introduction

In recent years, awareness of the danger posed by pollution of various environmental components (water, air, soil, etc.) has become a reality that concerns all social and industrial actors.

In Niger, the dyeing techniques used in the textile industry have contributed significantly to water pollution. This pollution is due to the discharge of organic and inorganic contaminants that are harmful to human health and ecosystems. To this end, effluent discharges from the textile industry are known for their intense coloration due to the presence of dyes, which are never 100 % exhausted from the dye baths; a quantity always remains in the effluent. The discharge of these effluents poses a major danger to humans and the environment. It is therefore essential to limit this pollution by implementing a dye removal technique adapted to our country (Niger). There are various methods for removing chemicals (heavy metals, dyes, phenols, etc.) from effluents. Among these methods, adsorption on porous

* Corresponding author: AMADOU KIARI Mahamane Nassirou

materials is one of the most widely used techniques [1–9]. It is a solid-fluid extraction process that requires an adsorbent (solid) and an adsorbate (liquid or gas). Microporous adsorbents are widely used in the extraction of chemical species in aqueous or gaseous phases due to their excellent adsorption capacity. This capacity is linked to the large specific surface area and porosity of the adsorbents [10,11]. Natural phosphates and activated carbons have been the subject of much research in the search for adsorbent materials. They are of interest in the treatment of industrial wastewater [1].

Phosphates have a wide range of physical, chemical, and textural properties. They are capable of forming bonds with organic molecules of various sizes. Recent studies have shown that these materials, whether natural or synthetic, can remove organic compounds from wastewater [1]. Activated carbon consists mainly of carbonaceous material with a porous structure. It can be produced from any carbon-rich raw material [12]. Nowadays, various studies have focused on the production and characterization of activated carbons from several types of plant-based materials such as: the shell of *Balanites aegyptiaca*, the shell of *Zizyphus mauritiana*, the shell of *Hyphaene thebaica* [13], the branches or petioles of the rônier palm [8,9], bamboo stems or canes [14], coconut [15], *eucalyptus* wood [16], the shells of *Tieghmelia*, known as makoré, and *Delonix*, known as flamboyant [17], the shells of *Parinari macrophylla* [18], and coffee residues [19].

It is in this context that our work fits in, the overall objective of which is to conduct a comparative study of the dye adsorption properties of natural phosphate from Tahoua and activated carbons. The latter are produced from the shell of the *Hyphaene thebaica* kernel by chemical activation with orthophosphoric acid.

2. Materials and methods

2.1. Phosphate

Figure 1 shows the raw natural phosphate powder from Tahoua, and Figure 2 shows the processed natural phosphate powder from Tahoua.

Figure 1 Raw natural phosphate powder from Tahoua

Figure 2 Processed natural phosphate powder from Tahoua

2.2. Shells of biomass used

The shells of *Hyphaene thebaica* (Figure 3a) were used to prepare activated carbon. These were collected from the waste dump of a local market called Katako (Niamey, Niger). They were crushed, washed with tap water to remove dust, rinsed with distilled water, and then dried in an oven at 105 °C for 24 hours (Figure 3b).

(a) (b)

Figure 3 *Hyphaene thebaica* shells (a) and crushed shells (b)

2.3. Reagents used

The reagents used in this work are presented in Table 1.

Table 1 Chemicals use

Chemicals	Mollir mass (g/mol)	Put (%)	Sources
Orthophosphorique Acid (H_3PO_4)	98	85 %	Merck
Methylene bleu ($C_{16}H_{18}Cl_3S$)	319.86	-	Sigma-Aldrich
Sodium thiosulfate ($Na_2S_2O_3.5H_2O$) Iodine	248.18 126.9	99 % -	Sigma-Aldrich Sigma-Aldrich

3. Methodology

3.1. Phosphate processing

Calcination is used to enrich the orthophosphate (P_2O_5) content and reduce the organic carbon and carbon dioxide content in phosphates. The principle of this process is to heat the natural phosphate powder from Tahoua to a high temperature of 850 °C for 2 hours [20].

3.2. Characterization of biomass

3.2.1. Moisture content and volatile matter content

Moisture content and volatile matter content were determined in accordance with AFNOR XP CEN/TS 14774 and AFNOR XP CEN/TS 15148 standards, respectively [6,21]. First, porcelain crucibles of mass P containing 2 g of biomass were dried in an oven at 105 °C for 24 hours. After cooling in a desiccator, the crucibles were weighed again. To determine the volatile matter content, the dried samples were placed in a muffle furnace at 1000°C for 3 hours. After cooling in a desiccator, the whole batch was weighed. The moisture content (H) and volatile matter content (PF) are given by expressions 1 and 2 respectively.

$$(H) = \frac{P_1 - P_2}{P_1 - P} \times 100 \quad \ldots\ldots \quad (1)$$

$$(P.F) = \frac{P_2 - P_3}{P_2 - P} \times 100 \quad \ldots\ldots \quad (2)$$

Where P_1 and P_2 are the masses of the crucible + sample before and after drying in the oven; P_3 is the mass of the whole after carbonization in the furnace.

3.2.2. Ash content

The ash content was determined in accordance with standard AFNOR XP CEN/TS 14775 [6,21]. In a porcelain crucible with an empty mass m_1, 1 g of biomass ground to a particle size of less than 200 µm was introduced. The sample was mineralized at 815 °C using a muffle furnace for 2 hours. After cooling in a desiccator, the whole thing (sample + crucible) was weighed to get the mass m_3.

The ash content is given by the following equation:

$$(\%C) = \frac{m_3 - m_1}{m_2 - m_1} \times 100 \quad \ldots\ldots \quad (3)$$

With m_2, the mass of the crucible + sample before mineralization.

3.2.3. Apparent density

To determine the apparent density, a 50 cm^3 test tube with an empty mass m1 was filled with biomass ground to a particle size of less than 200 µm, and the mass m_2 was recorded [6,21].

The density is given by the equation

$$\rho = \frac{m_2 - m_1}{V} \quad \ldots\ldots \quad (4)$$

3.3. Production of activated carbon

3.3.1. Preparation of activated carbon

The method used to prepare activated carbon is chemical activation [22–25]. The pretreated biomass is impregnated with two solutions of H_3PO_4 at 10 % and 40 %, at a rate of 20 g of biomass per 100 ml of solution. Impregnation is carried out under magnetic stirring for 24 hours at atmospheric pressure and room temperature. The samples were then filtered on ashless Büchner filter paper, washed with distilled water, and dried in an oven at 105 °C for 24 hours. After removal from the oven, the samples were cooled in a desiccator for 15 minutes. Once dried, each impregnated sample was placed in a crucible with a lid, and the assembly was placed in a muffle furnace at a temperature of 450 °C, with a heating rate of 2.66 °C/min and an isothermal plateau of 90 min at the end of pyrolysis. After the 90-minute plateau at the final pyrolysis temperature, the crucible was removed from the oven and cooled in a desiccator for 15 minutes. After cooling, the charcoal was washed thoroughly with distilled water to remove impurities until the pH was close to neutral, then dried in an oven at 105°C. The activated carbons thus obtained were ground and then sieved to obtain grains of a size less than or equal to 500 µm.

3.4. Characterization

3.4.1. Mass yield after pyrolysis

This is an important quantitative characteristic of activated carbon that reflects the loss of biomass mass during pyrolysis.

The following formula gives the expression for mass yield

$$\text{Yield} = \frac{m_f}{m_i} \times 100 \quad \ldots\ldots \quad (5)$$

final mass (mf) and initial mass (mi).

3.4.2. Surface function

The acid and base functions on the surface of activated carbons were determined and quantified using the Boehm titration method [26]. (Boehm, 1994). To determine these functions, 0.2 g of AC were brought into contact with 20 mL of each of the following solutions: NaOH, Na_2CO_3, $NaHCO_3$, C_2H_5ONa, and HCl at 0.1 M. Each solution was stirred for 24 hours to ensure that a maximum amount of the surface groups of AC reacted, then filtered; after filtration, 10 mL of each of the five solutions was measured. The basic solutions are titrated with 0.1 M hydrochloric acid using three drops of

bromothymol blue, phenolphthalein, bromocresol green, and helianthin as color indicators, respectively, and the acid solution is titrated with 0.1 M sodium hydroxide using bromothymol blue as the color indicator.

The quantification of acid and base groups is performed using the following formula

$$n_{éqR} = N_i V_i - N_f V_f \quad \ldots\ldots \quad (6)$$

nor is the number of equivalent grams that reacted; Nivi is the number of equivalent grams before the reaction; NV is the number of equivalent grams after the reaction.

3.4.3. pH at zero charge point (pH_{PZC})

The pH at zero charge point (pH_{PZC}), which allows the net charge of the material surface to be determined, was calculated using the method described by Ousmaila et al., [5]. This method involves preparing 0.1 M sodium chloride (NaCl) solutions at different pH values, namely 2, 4, 6, 8, and 10. The pH values were adjusted with a pH meter using sodium hydroxide and hydrochloric acid solutions. In a 50 mL beaker, 0.1 g of CA was mixed with 20 mL of each solution. The mixture was stirred magnetically for 72 hours. The suspension was filtered through filter paper and the pH of the filtrate was measured. Then, the $pH_f = f(pH_i)$ curve was plotted. The intersection point between this curve and the first bisector gives the pH at the zero-loading point of the activated carbon in question.

pHf: final pH and pHi: initial pH.

3.5. Adsorption of micropollutants

3.5.1. Iodine index

The iodine index is an important characteristic in the evaluation of the micropores of activated carbon. In this study, it was determined using the method applied by GUEYE [16]. Thus, a volume of 20 mL of a 0.02 N iodine solution was brought into contact with 0.2 g of activated carbon for 4 min. The treated solution was filtered, and then 10 mL of filtrate was titrated with a 0.1 N sodium thiosulfate solution in the presence of a few drops of starch paste. Finally, the iodine index (I_d) expressed in mg/g was calculated using equation (7).

$$I_d = \frac{(C_0 - \frac{C_{thio} V_{thio}}{2V_{I2}}) M I_2 V_{ads}}{m_{ca}} \quad \ldots\ldots \quad (7)$$

Where, I_d: adsorption capacity of I_2; C_0: initial concentration of the I_2 solution (in mol/L); C_{thio}: concentration of $Na_2S_2O_3$ (in mol/L); V_{thio}: volume of $Naso_3$ at equivalence (in mL); V_{I2}: volume of iodine titrated (in mL); MI_2: molar mass of I_2 (in g/mol); Vads: adsorption volume (in mL); m_{ca}: mass of adsorbent used (in g).

adsorption volume (in mL); mica: mass of adsorbent used (in g).

3.5.2. Methylene Blue (MB) Index

The MB index, expressed in mg. g^{-1}, represents the adsorption capacity of medium-sized molecules for the purpose of evaluating mesopores and macrospores.

a) Preparation of standard MB test solution

Place 1.2 g of MB in a 1 L volumetric flask. Fill the flask with distilled water to the mark. The solution is left to stand for approximately one night. The solution is then tested by adding 0.25 % acetic acid (i.e., 5.0 ml per 1 L of solution). For this purpose, a test solution was prepared by dilution corresponding to an absorbance of 0.840 ± 0.01 at a wavelength of 620 nm.

b) Procedure for determining the MB index

Methylene blue adsorption tests were performed using the CEFFIC protocol [5,6]. In a 250 mL Erlenmeyer flask, we added 100 mg of adsorbent to 100 mL of standard MB solution. The mixture was stirred for 20 min. After stirring, the mixture was filtered and the residual concentration of methylene blue was measured at $\boldsymbol{\lambda}$ = 620 nm using a UV-visible spectrophotometer.

The methylene blue index is given by:

$$I_{BM} = \frac{(C_i - C_r)VM}{m} \times 100 \quad \ldots\ldots \quad (8)$$

With I_{BM}: adsorption capacity of CA (in mg/g); Ci: initial concentration of BM solution (in mol/L); Cr: residual concentration of BM solution (in mol/L); V: volume of BM solution (in mL); M: molar mass of BM; m: mass of adsorbent used (in g)

3.6. Methyl orange (MO) adsorption kinetics

In a 500 mL beaker, 200 mL of methyl orange (MO) solution with an initial concentration of 50 mg/L and 80 mg of adsorbent are added. This mixture is stirred at 25 °C. At regular intervals, 1 mL of the mixture was sampled and filtered using a 0.45 µm pore size filter paper. A JENWAY 6305 UV-visible spectrophotometer was used to measure the residual MO concentration at a wavelength of 520 nm. The quantities adsorbed at equilibrium (Qe) were calculated using equation 9.

$$Q_e = \frac{(C_i - C_r)}{m} \times V \quad \ldots\ldots \quad (9)$$

Where Ci and Cr are the initial and residual concentrations of methyl orange (in mg. L-1); V is the volume (in L) of the solution used for the adsorption tests; and m is the mass (in g) of adsorbent.

4. Results and discussion

4.1. Characterization of biomass

The composition and physical properties of biomass are parameters that influence its conversion into activated carbon [13]. Table 2 summarizes the results of the immediate analysis performed on the shell of *Hyphaene thebaica* (HT).

Table 2 Immediate analysis results

Biomass	Moisture content (%)	Ash content (%)	Carbon content (%)	Actual density g/cm³
Hyphaene thebaic (HT)	5.0026	5.8286	74.850	0.3220

Table 2 shows that the ash content of biomasses is less than 6 %. This indicates that these biomasses can be used to produce activated carbons with large specific surface areas [8] .This parameter has a significant effect on the quality of activated carbon. It is also known that high ash content reduces the specific surface area of activated carbons [13,16]. In fact, ash intercalates into the carbon structure, clogs the pores, and reduces the porosity of the activated carbon. Unlike the moisture and ash content, which are relatively low, the carbon content is very high, at around 74.85 %. Biomass is therefore mainly composed of organic matter. Such volatile matter values are a good indicator for obtaining activated carbon with a high degree of graphitization, a high gross calorific value (GCV), and sufficient functional groups [13,16].

4.1.1. Mass yield

The mass yield results after pyrolysis are shown in Table 3.

Table 3 Mass yield results after pyrolysis of CAs

Biomass	**H_3PO_4 concentration (%)**	**Impregnation time (h)**	**Pyrolysis temperature (°C)**	**Heating rate °C/min**	**Carbonization time (h)**	**Mass yield (%)**
Hyphaene thebaica	10	24	450	2.66	1 h 30	42.85
	40	24	450	2.66	1 h 30	47.05

These results show that increasing the concentration of the activating agent H_3PO_4 increases the mass yields after pyrolysis of CAs. This can be explained by the fact that H_3PO_4, as an activating agent, is a dehydrating agent that delays thermal decomposition, limits the loss of volatile matter, and leads to the formation of a rigid carbon matrix [5,21].

4.1.2. Surface functions

Table 4 shows the mEq/g content of the adsorbents' functions.

Table 4 Surface function of adsorbents

Adsorbent	**carboxylic**	**lactone**	**phenol**	**carbonyl**	**Total acid**	**Basic total**
CA-HT 10 %	1.2	1.3	3.2	2.4	8.1	-
CA-HT 40 %	1.5	2.1	2	2.1	7.7	-

As expected, with this acid chemical activation, the CA-HT 10% and CA-HT 40% activated carbons produced contain a large amount of acid groups and no basic groups. This can be explained by the fact that the ACEs were not exposed to oxygen below 200°C or above 700°C, they did not undergo hydrogen treatment, and they were not degassed at room temperature, as this is the stage at which basic functions are introduced. Similar results have been reported in the literature [5,21]. These acidic surface groups are probably due to polyphosphates bound to the surface of the carbon and to carboxylic groups. Orthophosphoric acid acts as a catalyst by promoting bond cleavage reactions and facilitating cross-linking via cyclization, condensation, and the formation of phosphate and polyphosphate bonds [27]. Carbonyl and phenolic groups predominate on their surface.

4.1.3. pH at zero charge point (pH_{PCN})

Figures 4, 5, and 6 show the pH determination curves at zero charge point for activated carbons activated with orthophosphoric acid and natural phosphate from Tahoua, respectively.

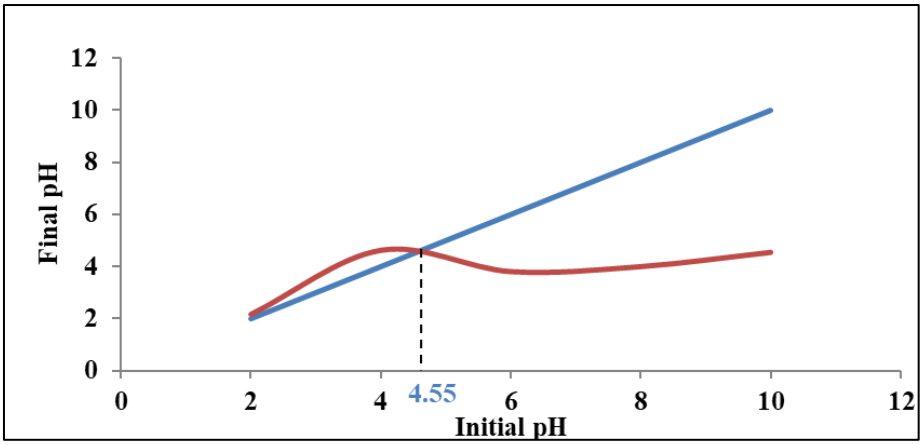

Figure 4 Determination of the pH_{PCN} of CA HT 10% activated with H_3PO_4

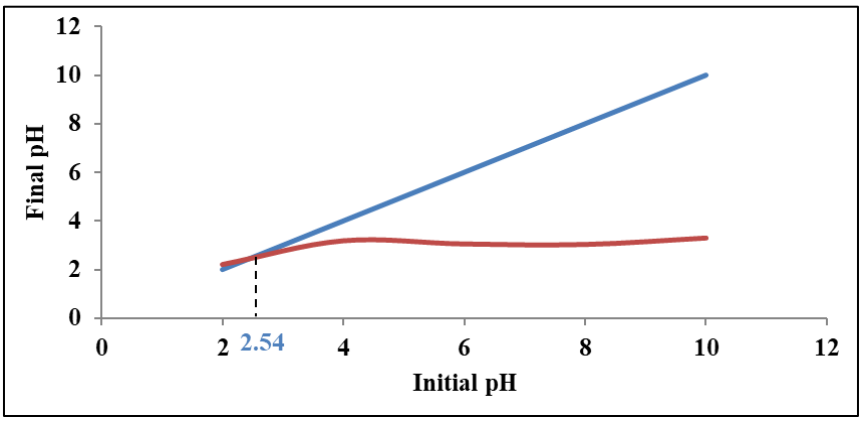

Figure 5 Determination of the pH_{PCN} of CA HT 40 % activated with H_3PO_4

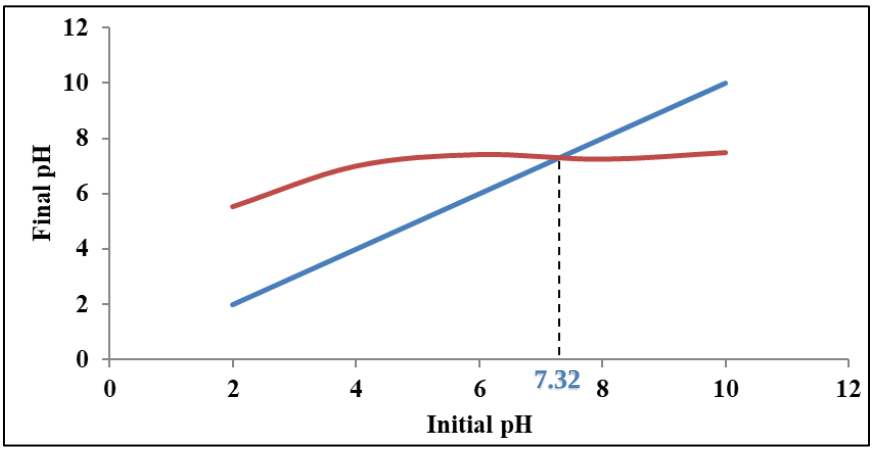

Figure 6 Determination of the pH_{PCN} of PNT

The pH values at the zero charge point of activated carbons are all below neutrality (pH < 7). They range from 2.54 to 4.55. Similar results have been observed in other studies [27,28]. At a pH higher than these values, the surface of the activated carbon is negatively charged, whereas it is positively charged at a pH lower than the pHpcn. As for PNT, the

pH value at the zero-charge point is close to neutrality at 7.32. At a pH higher than this value, the surface of PNT is negatively charged, whereas it is positively charged at a pH lower than the pHpcn.

4.2. Adsorption of micropollutants

4.2.1. Iodine index

The iodine index results for the activated carbons produced and the natural phosphate from Tahoua are shown in Table 5.

Table 5 Iodine index results in mg/g

	PNT	**CA HT 10 %**	**CA HT 40 %**
V_{thio} (mL)	3	0.7	0.1
Q_{I2}	126.90	418.77	494.91

In the case of CAs, the results show that the parameter influencing the iodine index is the concentration of the activating agent (H_3PO_4). Several authors have shown that the iodine index increases with the concentration of the activating agent [4,21,29]. These results are similar to those obtained by [4,21].

For phosphate, the adsorption capacity of I_2 is lower than that of the two (2) ACs. This could be due to the fact that raw natural phosphate from Tahoua has been found to be a material with moderate adsorption affinity compared to activated carbons for iodine removal.

4.2.2. Determination of the Methylene Blue (MB) index

The MB results for the activated carbons produced and the natural phosphate from Tahoua are shown in Table 6

Table 6 Methylene blue index results in mg/g

Adsorbent	**PNT**	**CA HT 10%**	**CA HT 40%**
BM index	548.879	810.01	886.72

It can be seen that the adsorption capacity of BM by CA increases with the concentration of the activating agent (H_3PO_4). These results are similar to those obtained by [4,21].

For PNT, the adsorption capacity value obtained for BM is relatively low compared to those obtained by ACs. This could be due to the fact that raw Tahoua natural phosphate has been found to be a material with moderate adsorption affinity compared to activated carbons for BM removal.

4.2.3. Methyl orange contact time

The kinetic study allows us to determine the contact time required to reach adsorption equilibrium. To do this, we monitored the adsorption kinetics of MO for an initial concentration of 50 mg/L, with a mass of 80 mg of adsorbent.

The results of the adsorption kinetics of MO on the adsorbents are presented in Figures 7

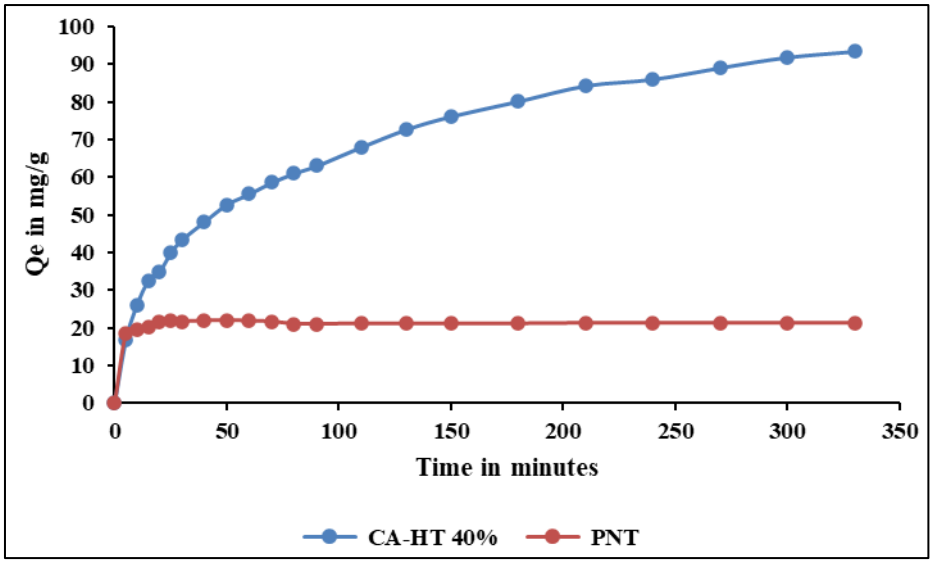

Figure 7 Variation in contact time CA HT 40% and PNT (Ci = 50 mg/L, m = 80 mg)

These curves show the variation in the amount of MO adsorbed (Qe) by the adsorbents over time. The results obtained show that equilibrium is reached much more quickly with Tahoua natural phosphate, after 25 minutes, than with activated carbon, after 40 minutes. However, the quantities adsorbed with PNT are lower than those obtained with CA-HT 40 %. They are 21.82 mg/g for PNT and 48.12 mg/g. This indicates that activated carbon adsorbs methyl orange better than Tahoua natural phosphate.

5. Conclusion

The objective of this study was to conduct a comparative study of dye adsorption on natural phosphate from Tahoua and activated carbon. The characterization of biomass on the shell of the *Hyphaene thebaica* (HT) kernel yielded the following results: moisture content of 5.002 % and ash content of 5.828 %. These values are very low, while the volatile matter content (loss on ignition) is very high at 98.958 %; the mass yield after pyrolysis was around 42.85 % and 47.05 % respectively for the HT shell impregnated with H_3PO_4 at 10 % and 40 %. After characterizing *Hyphaene thebaica* (HT) shells, a study focused on the preparation of activated carbons. The performance of these materials was evaluated in terms of the iodine index, methylene blue index, and methyl orange index. The adsorption capacities of diiodine (I_2) obtained with activated carbons are greater than those obtained with natural phosphate from Tahoua; the adsorption capacities of methylene blue (MB) obtained with activated carbons are greater than those obtained with natural phosphate from Tahoua; the surface functions of ACEs are acidic in nature; the pH at the zero charge point of CAEs is all below neutrality, but for PNT, it is slightly above neutrality; the influence of contact time on methyl orange (MO) retention gave the following results: for 40 % activated CAE, the contact time is 40 minutes, the mass of adsorbent is 80 mg, and the initial concentration of the solution is 50 mg/L. The contact time for PNT is around 25 minutes.

Compliance with ethical standards

Acknowledgments

We would like to thank Abdou Moumouni University in Niamey for providing us with the setting in which the work was carried out.

Disclosure of conflict of interest

The authors declare no conflicts of interest regarding the publication of this paper.

References

[1] N. BARKA, Etude comparative des propriétés d'adsorption de quelques micro-polluants sur les phosphates naturels et le charbon actif., 2004.

[2] M.N.A. Kiari, G.D. Fanou, A.T. Sylvie, A. Ouattara, H. Kone, M.M.M. Alma, E.N. Assidjo, K.B. Yao, Process conditions optimization of plant waste-derived microporous activated carbon using a full factorial design and genetic algorithm, (2022).

[3] M.N. Amadou Kiari, A.T.S. Konan, O. Sanda Mamane, L.Y. Ouattara, M.H. Ibrahim Grema, M. Siragi Dounounou Boukari, A. Adamou Ibro, M.M. Malam Alma, K.B. Yao, Adsorption kinetics, thermodynamics, modeling and optimization of bisphenol A on activated carbon based on *Hyphaene thebaica* shells, Case Studies in Chemical and Environmental Engineering 10 (2024) 100903. https://doi.org/10.1016/j.cscee.2024.100903.

[4] O.S. Mamane, M.S.D. Boukari, A.R. Chaibou, Valorisation de coques de noix de Balanites aegyptiaca (L.) Del. et élimination du Chrome en solution, (2018) 15.

[5] S.M. Ousmaila, S.D.B. Maâzou, M.A.M. Mousbahou, N. Ibrahim, Valorisation des coques de noyaux de Balanites aegyptiaca (L.) Del. et *Hyphaene thébaica* (L.) Mart. pour l'élaboration et caractérisation de Charbons Actifs; application pour l'élimination du chrome, ESJ 14 (2018) 195. https://doi.org/10.19044/esj.2018.v14n21p195.

[6] O.S. Mamane, A. Zanguina, I. Daou, I. Natatou, Préparation et caractérisation de charbons actifs à base de coques de noyaux de Balanites Eagyptiaca et de Zizyphus Mauritiana, (2016) 10.

[7] B.G.H. Briton, B.K. Yao, Y. Richardson, L. Duclaux, L. Reinert, Y. Soneda, Optimization by Using Response Surface Methodology of the Preparation from Plantain Spike of a Micro-/Mesoporous Activated Carbon Designed for Removal of Dyes in Aqueous Solution, Arab J Sci Eng 45 (2020) 7231–7245. https://doi.org/10.1007/s13369-020-04390-0.

[8] H. Koné, K.E. Kouassi, A.S. Assémian, K.B. Yao, P. Drogui, Investigation of breakthrough point variation using a semi-industrial prototype packed with low-cost activated carbon for water purification, (2021) 20.

[9] A.T.S. Konan, R. Richard, C. Andriantsiferana, K.B. Yao, Recovery of borassus palm tree and bamboo waste into activated carbon: application to the phenolic compound removal, (2020) 15.

[10] M. Siragi D B, I. Natatou, V. Dubois, Synthesis of activated carbon from Balanites aegyptiaca and hyphaene thebaica shells by physical activation, Carbon Trends 21 (2025) 100555. https://doi.org/10.1016/j.cartre.2025.100555.

[11] Maâzou Siragi D. B., Halidou I. Hima, Grégory Ploegaerts, Ousmaila Sanda Mamane, Vincent Dubois, Ibrahim Natatou, Modelling of the kinetics adsorption of gold (I) cyanide complex ion by active carbons prepared from Parinari macrophylla shells, World J. Adv. Res. Rev. 15 (2022) 394–406. https://doi.org/10.30574/wjarr.2022.15.3.0941.

[12] M.N. Amadou Kiari, A.T.S. Konan, O. Sanda Mamane, H. Kone, G.D. Fanou, M. Siragi Dounounou Boukari, M.H. Ibrahim Grema, M.M. Malam Alma, K.B. Yao, Influence of Orthophosphoric Acid Activation on the Quality of Activated Carbons, MSF 1122 (2024) 91–98. https://doi.org/10.4028/p-kd7gN9.

[13] O. Sanda Mamane, Valorisation de déchets agro-alimentaires pour l'élaboration de charbons actifs ; caractérisation et application dans la dépollution des eaux usées chargées en chrome issues de la Tannerie Malam Yaro de Zinder-Niger, These de Doctorat Chimie Minerale de Metaux, Université Abdou Moumouni de Niamey, 2019.

[14] A.T.S. Konan, Couplage adsorption/procédé d'oxydation avancée pour l'élimination du 2,4-diméthylphénol en milieu aqueux, These en Genie des Procedés, Institut National Felix HOUPHOUET BOIGNY et Université de Toulouse, 2019.

[15] D. Bamba, Elimination du diuron des eaux par des techniques utilisant les ressources naturelles de la cote d'Ivoire : photocatalyse solaire et charbon actif de coques de noix de coco, These de Doctorat Chimie-Physique, Université de Cocody Abijan, 2009.

[16] M. baye Gueye, Développement de charbon actif a partir de biomasses lignocellulosiques pour des applications dans le traitement de l'eau, These de Doctorat en Energie, Institut International de l'Ingenierie de l'Eau et de l'Environnement, 2015.

[17] N. Aboua Kouassi, Optimisation par le plan Factoriel complet des conditions de production de charbon actif et utilisation pour l'élimination de colorant et métaux lourds en solutions aqueuses, These de Doctorat Chimie-Physique, Université Felix HOUPHOUET BOIGNY, 2013.

[18] M. Siragi D. B., D. Desmecht, H.I. Hima, O.S. Mamane, I. Natatou, Optimization of Activated Carbons Prepared from <i>Parinari macrophylla</i> Shells, MSA 12 (2021) 207–222. https://doi.org/10.4236/msa.2021.125014.

[19] K.K. Naganathan, A.N.M. Faizal, M.A.A. Zaini, A. Ali, Adsorptive removal of Bisphenol a from aqueous solution using activated carbon from coffee residue, Materials Today: Proceedings 47 (2021) 1307–1312. https://doi.org/10.1016/j.matpr.2021.02.802.

[20] E. El Ouardia, Étude de la calcination du phosphate clair de youssoufia (Maroc), Afrique Science: Revue Internationale des Sciences et Technologie 4 (2010). https://doi.org/10.4314/afsci.v4i2.61676.

[21] S.D.B. Maazou, H.I. Hima, M.M. Malam Alma, Z. Adamou, I. Natatou, Elimination du chrome par du charbon actif élaboré et caractérisé à partir de la coque du noyau de Balanites aegyptiaca, Int. J. Bio. Chem. Sci 11 (2018) 3050. https://doi.org/10.4314/ijbcs.v11i6.39.

[22] O. Oginni, K. Singh, G. Oporto, B. Dawson-Andoh, L. McDonald, E. Sabolsky, Influence of one-step and two-step KOH activation on activated carbon characteristics, Bioresource Technology Reports 7 (2019) 100266. https://doi.org/10.1016/j.biteb.2019.100266.

[23] O. Oginni, K. Singh, G. Oporto, B. Dawson-Andoh, L. McDonald, E. Sabolsky, Effect of one-step and two-step H3PO4 activation on activated carbon characteristics, Bioresource Technology Reports 8 (2019) 100307. https://doi.org/10.1016/j.biteb.2019.100307.

[24] A. Supong, P.C. Bhomick, M. Baruah, C. Pongener, U.B. Sinha, D. Sinha, Adsorptive removal of Bisphenol A by biomass activated carbon and insights into the adsorption mechanism through density functional theory calculations, Sustainable Chemistry and Pharmacy 13 (2019) 100159. https://doi.org/10.1016/j.scp.2019.100159.

[25] H.N. Tran, S.-J. You, H.-P. Chao, Fast and efficient adsorption of methylene green 5 on activated carbon prepared from new chemical activation method, Journal of Environmental Management 188 (2017) 322–336. https://doi.org/10.1016/j.jenvman.2016.12.003.

[26] H.P. Boehm, Some aspects of the surface chemistry of carbon blacks and other carbons, Carbon 32 (1994) 759–769. https://doi.org/10.1016/0008-6223(94)90031-0.

[27] N.V. Sych, S.I. Trofymenko, O.I. Poddubnaya, M.M. Tsyba, V.I. Sapsay, D.O. Klymchuk, A.M. Puziy, Porous structure and surface chemistry of phosphoric acid activated carbon from corncob, Applied Surface Science 261 (2012) 75–82. https://doi.org/10.1016/j.apsusc.2012.07.084.

[28] A. Ould-Idriss, M. Stitou, E.M. Cuerda-Correa, C. Fernández-González, A. Macías-García, M.F. Alexandre-Franco, V. Gómez-Serrano, Preparation of activated carbons from olive-tree wood revisited. I. Chemical activation with H3PO4, Fuel Processing Technology 92 (2011) 261–265. https://doi.org/10.1016/j.fuproc.2010.05.011.

[29] I. Tchakala, L. Bawa, G. Djaneye-Boundjou, K. Doni, P. Nambo, Optimisation du procédé de préparation des Charbons Actifs par voie chimique (H3PO4) à partir des tourteaux de Karité et des tourteaux de Coton, Int. J. Bio. Chem. Sci 6 (2012) 461–478. https://doi.org/10.4314/ijbcs.v6i1.42.